


Cosmic Strings from Thermal Inflation

Robert Brandenberger *  and Aline Favero

Department of Physics, McGill University, Montréal, QC H3A 2T8, Canada; aline.favero@mail.mcgill.ca

* Correspondence: rhb@physics.mcgill.ca

Abstract: Thermal inflation was proposed as a mechanism to dilute the density of cosmological moduli. Thermal inflation is driven by a complex scalar field possessing a large vacuum expectation value and a very flat potential, called a “flaton”. Such a model admits cosmic string solutions, and a network of such strings will inevitably form in the symmetry breaking phase transition at the end of the period of thermal inflation. We discuss the differences of these strings compared to the strings which form in the Abelian Higgs model. Specifically, we find that the upper bound on the symmetry breaking scale is parametrically lower than in the case of Abelian Higgs strings, and that the lower cutoff on the string loop distribution is determined by cusp annihilation rather than by gravitational radiation (for the value of the transition temperature proposed in the original work on thermal inflation).

Keywords: thermal inflation; cosmic strings; early universe

1. Introduction

Thermal inflation (not to be confused with *warm inflation* [1]) was proposed [2] as a mechanism to dilute the number density of unwanted moduli quanta or gravitinos. Moduli fields are predicted in many models beyond the particle physics Standard Model (an example being scalar fields corresponding to the radii of the extra spatial dimensions which superstring theory requires). In such models, moduli quanta are often left over from the Big Bang period, produced at the end of a phase of primordial inflation, or generated during a compactification phase transition. If they are heavy (as they typically are in models in which the energy scale of the new physics is high—e.g., of the string scale), then they would rapidly come to dominate the universe long before the time of nucleosynthesis and would lead to severe cosmological problems. Similarly, if the scale of supersymmetry breaking is high, the gravitinos would have a large mass and would lead to a similar problem [3,4]. The proposal of [2] is to dilute the number density of moduli by invoking a period of inflation (in such a period the energy density in the moduli fields would decrease exponentially compared to the total energy density which is dominated by that of the thermal inflation field). This period should be sufficiently long to dilute the moduli, but short enough not to redshift the fluctuations which are generated in the primordial universe.

Thermal inflation is generated by adding a new matter sector involving a complex scalar field¹ ϕ with a symmetry breaking potential $V(\phi)$, and gauging the resulting $U(1)$ symmetry (this gauging is performed since there is evidence that global symmetries are inconsistent with quantum gravity [6]). Thermal inflation is assumed to occur in the radiation phase of cosmology. Thermal effects are assumed to trap ϕ at the symmetric point $\phi = 0$. At a temperature T_i given by

$$V(0) = T_i^4, \quad (1)$$

the potential energy of ϕ begins to dominate and inflation begins. The coupling of ϕ to the thermal bath generates a finite temperature contribution to the effective potential

$$V_T(\phi) = V(\phi) + gT^2\phi^2, \quad (2)$$



Citation: Brandenberger, R.; Favero, A. Cosmic Strings from Thermal Inflation. *Universe* **2024**, *10*, 253. <https://doi.org/10.3390/universe10060253>

Academic Editor: Kazuharu Bamba

Received: 13 May 2024

Revised: 30 May 2024

Accepted: 31 May 2024

Published: 4 June 2024



Copyright: © 2024 by the authors. Licensee MDPI, Basel, Switzerland. This article is an open access article distributed under the terms and conditions of the Creative Commons Attribution (CC BY) license (<https://creativecommons.org/licenses/by/4.0/>).

where g is the coupling constant describing the interactions between ϕ and the thermal bath². At a temperature T_c when the positive contribution to the curvature of the potential at $\phi = 0$ equals the absolute value of the (negative) curvature coming from the bare potential $V(\phi)$, symmetry breaking sets in, ϕ rolls to the bottom of its potential, and thermal inflation ends. In order to generate the required hierarchy between T_c and T_i , it was assumed that the bare potential $V(\phi)$ contains no quartic term. The hierarchy between T_i and T_c determines the number N of e-foldings of thermal inflation

$$\frac{T_c}{T_i} = e^{-N}. \tag{3}$$

Since the vacuum manifold of ϕ is S^1 , cosmic string defects inevitably form in the phase transition, which ends thermal inflation [10,11] (see [12–15] for reviews of the role of cosmic strings in cosmology). As the scale of symmetry breaking for thermal inflation is assumed to be of the order $m_0 \sim 10^2\text{--}10^3$ GeV, one might—based on intuition from Abelian Higgs strings [16]—have expected the signatures of these strings to be negligible. As we show here, thermal inflation strings have different properties compared to strings formed in the standard Abelian Higgs model. For the same value of the symmetry breaking temperature, thermal inflation strings have a parametrically larger mass per unit length than regular strings. Comparing strings with the same mass per unit length μ , thermal inflation strings have a parametrically greater width than regular strings. These differences affect the distribution of string loops, and hence, the observational consequences of the strings (see, e.g., [17] for a short review) need to be revisited³.

In this article, we use natural units in which the speed of light, Planck’s constant, and Boltzmann’s constant are set to 1. The Planck mass is denoted by m_{pl} . The mass per unit length of a string will be denoted by μ , or often in terms of the dimensionless quantity $G\mu$, where G is Newton’s gravitational constant.

2. Thermal Inflation Strings

The thermal inflation model [2] assumes a potential given by

$$V(\phi) = V_0 - m_0^2|\phi|^2 + \sum_{n=1}^{\infty} \frac{\lambda_n|\phi|^{2n+4}}{m_{pl}^{2n}}, \tag{4}$$

where V_0 is tuned such that the potential energy in the vacuum manifold vanishes. The λ_n are dimensionless coupling constants, and the mass scale m_0 determines the (negative) curvature of the potential at the origin. We shall consider a simplified potential containing only the $n = 1$ term (the contributions from the terms with $n > 1$ are Planck suppressed for the questions we are asking, i.e., those involving small field values)⁴. Thus, we consider the potential

$$V(\phi) = V_0 - m_0^2|\phi|^2 + \lambda|\phi|^6 m_{pl}^{-2}. \tag{5}$$

This potential is to be compared with the potential for the Abelian Higgs model which is

$$V_{AH}(\phi) = \frac{\lambda_{AH}}{4} (|\phi|^2 - \eta^2)^2, \tag{6}$$

where η is the value of $|\phi|$ in the vacuum manifold, and λ_{AH} is a dimensionless coupling constant. The key difference between the thermal inflation potential and the potential in the Abelian Higgs model is the absence of the quartic term in the former. This leads to a different scaling of properties of a thermal inflation string as a function of m_0 .

As we will see below, the hierarchy between T_i and T_c increases as m_0 decreases. To obtain an e-folding number $N \sim 10$ of thermal inflation, a value of $m_0 \sim 10^2\text{--}10^3$ GeV was suggested [2].

From (5), it immediately follows (by finding the value of ϕ for which the derivative of V vanishes) that the value η of $|\phi|$ which minimizes the potential is given by

$$\eta^2 = \left(\frac{1}{3}\right)^{1/2} \lambda^{-1/2} \frac{m_{pl}}{m_0} m_0^2 \tag{7}$$

which is parametrically larger by a factor of m_{pl}/m_0 than what is obtained for an Abelian Higgs string given the same value of the curvature of the potential at $\phi = 0$. For the value of m_0 indicated above, η is of the order of 10^{10} GeV and not 10^2 GeV as it would be for an Abelian Higgs string with the same value of m_0 .

Demanding that the potential vanishes for $|\phi| = \eta$ yields

$$V_0 = \frac{2}{3} \left(\frac{1}{3}\right)^{1/2} \lambda^{-1/2} m_0^3 m_{pl} \tag{8}$$

which is also parametrically larger by a factor of m_{pl}/m_0 compared to the corresponding result for the Abelian Higgs string (taking coupling constants to be of the order 1). This leads to the fact that the temperature T_i corresponding to the onset of thermal inflation is parametrically larger than what one might have guessed from Abelian Higgs string intuition

$$T_i \sim \lambda^{-1/8} \left(\frac{m_{pl}}{m_0}\right)^{1/4} m_0. \tag{9}$$

On the other hand, the temperature at which the symmetry breaking phase transition takes place is given by

$$T_c \sim m_0, \tag{10}$$

setting g to be of the order 1. Comparing (9) and (10), we see that it is precisely the enhancement factor discussed above which allows for a period of thermal inflation to take place.

Let us now compare the width of a thermal inflation string with that of an Abelian Higgs string for the same value of the phase transition temperature T_c . The width is determined by minimizing the sum of the potential and gradient energy terms. Increasing the width of the string costs potential energy, while decreasing the width leads to an increase in the gradient energy. For a straight string centered at $r = 0$ (in polar coordinates), the field configuration of a string with winding number 1 can be written as

$$\phi(r, \theta) = f(r) \eta e^{i\theta}, \tag{11}$$

where the profile function $f(r)$ increases from $f(0) = 0$ to $f(r) = 1$ for $r > w$. The potential energy μ_p per unit length of the string can, hence, be estimated to be

$$\mu_p(w) \sim \pi w^2 V_0. \tag{12}$$

The scalar field angular gradient energy for a local string is cancelled by the gauge fields beyond a radius r_A which is set by the gauge field mass. For $r < w$, the angular gradient energy decays since $f(r)$ decays as r decreases. Hence, the mass per unit length μ_a from gradients can be estimated as

$$\mu_a(w) \sim 2\pi\eta^2 \int_w^{r_A} \frac{1}{r} f(r)^2. \tag{13}$$

It then follows from (13) that

$$\frac{\partial}{\partial w} \mu_a(w) \sim -2\pi\eta^2 \frac{1}{w}. \tag{14}$$

Hence, by minimizing the sum of potential and angular gradient energy (to first approximation the radial gradient energy does not depend on w), it follows that

$$w \sim V_0^{-1/2} \eta. \tag{15}$$

For Abelian Higgs strings, this yields

$$w_{AH} \sim \lambda^{-1/2} \eta^{-1}, \tag{16}$$

while for thermal inflation strings, it yields

$$w \sim m_0^{-1}. \tag{17}$$

In terms of the phase transition temperature, the widths of thermal inflation strings and Abelian Higgs strings are of the same order of magnitude. However, in terms of the mass per unit length, there is a parametric difference, and this difference will have important implications for the string loop distribution. From energy equipartition, the energy per unit length μ of a string is given by

$$\mu \sim w^2 V_0. \tag{18}$$

For Abelian Higgs strings, this yields

$$\mu_{AH} \sim \eta^2 \sim T_c^2, \tag{19}$$

while for thermal inflation strings, it yields

$$\mu \sim \lambda^{-1/2} \frac{m_{pl}}{m_0} T_c^2. \tag{20}$$

Thus, for a fixed mass per unit length, a thermal inflation string has a width

$$w \sim \lambda^{-1/2} \frac{m_{pl}}{\sqrt{\mu}} \mu^{-1/2}, \tag{21}$$

which is much greater than the width

$$w_{AH} \sim \lambda^{-1/2} \mu^{-1/2}. \tag{22}$$

of an Abelian Higgs string.

Comparing (19) and (20), we see that for a fixed symmetry breaking scale of $T_c \sim m_0 \sim 10^2$ GeV, an Abelian Higgs strings would have a mass per unit length of $G\mu_{AB} \sim 10^{-34}$, which is many orders of magnitude smaller than the range of values of $G\mu$, which can have interesting cosmological effects. In the case of thermal inflation strings, on the other hand, for the same value of T_c , we obtain $G\mu \sim 10^{-17}$, which is now approaching the range which is of interest for string signals in cosmological observations.

3. Thermal String Loop Distribution

The parametric enhancement of the width of a thermal inflation string compared to the width of an Abelian Higgs string with the same mass per unit length has important implications for the loop distribution.

The causality argument [10,11], which implies that the distribution of long strings (strings with a curvature radius comparable to and greater than the Hubble radius) takes on a scaling solution where the number of long string segments crossing any given Hubble volume is independent of time, applies equally to Abelian Higgs and thermal inflation strings. This *scaling solution* of the long string network is maintained by string loop production. As for Abelian Higgs strings, we can assume that the one scale loop production

model [22–24] also applies⁵ to thermal inflation strings, implying that at time t , loops are produced with radius $R = \alpha t$, where α is a constant that can be normalized by string evolution simulations which yield $\alpha \sim 10^{-1}$. Once produced, the number density $n(R, t)$ of loops in the radius interval between R and $R + dR$ redshifts. Thus, at times t after the time t_{eq} of equal matter and radiation, we have

$$\begin{aligned} n(R, t)dR &= NR^{-2}t^{-2}dR \quad \alpha t > R > \alpha t_{eq} \\ n(R, t)dR &= NR^{-5/2}t_{eq}^{1/2}t^{-2}dR \quad \alpha t_{eq} > R > R_{co}, \end{aligned} \tag{23}$$

where N is a constant determined by the number of long string segments per Hubble volume. R_{co} is a cutoff radius below which loops live for less than one Hubble time, and whose consequences for cosmology can be neglected⁶.

For non-superconducting strings, there are two main mechanisms by which string loops decay. The first is gravitational radiation: string loops have relativistic tension and, hence, oscillate and emit gravitational radiation. The power of gravitational radiation from a string loop of radius R is [33]

$$P_g = \gamma G\mu^2, \tag{24}$$

where γ is a constant of the order 10^2 . Gravitational radiation implies that loops with radius $R < R_g$ where

$$R_g = \gamma G\mu t \tag{25}$$

will live less than one Hubble expansion time, and hence, their cosmological effects are negligible.

Cusp evaporation is a second decay mechanism [34]. A cusp is a point on the string which moves at the speed of light. Strings have finite width, and around the cusp point, the string segments on either side of the cusp point overlap for a region of length⁷

$$l_c(R) \sim R^{1/2}w^{1/2}. \tag{26}$$

Locally the cusp region looks like a string–antistring pair, and there is no topology protecting the cusp region against annihilation into gauge and scalar field quanta. It can be proven that string loops described by the effective Nambu–Goto action have at least one cusp per oscillation time [36]. Hence, the power of the cusp annihilation process is

$$P_c \sim \frac{1}{R}l_c(R)\mu = \left(\frac{w}{R}\right)^{1/2}\mu. \tag{27}$$

From the above equation, it follows that, due to cusp evaporation, string loops with a radius less than

$$R_c = w^{1/3}t^{2/3} \tag{28}$$

live for less than one Hubble expansion time. The cutoff radius R_{co} in the loop distribution of (23) is the larger of R_g and R_c .

Comparing the strengths of gravitational radiation power (24) and cusp annihilation power (27), we see that the parametrically larger width of a thermal inflation string (for a given mass per unit length) will lead to a parametric amplification of the role of cusp annihilation compared to gravitational wave decay. We also see that the relative importance of cusp annihilation increases the lower the value of $G\mu$ is.

The condition for cusp annihilation to dominate over gravitational radiation is $R_c > R_g$ or

$$w > (\gamma G\mu)^3 t. \tag{29}$$

For Abelian Higgs strings, this yields

$$\left(\frac{T}{m_{pl}}\right)^2 > \lambda^{1/2}\gamma^3(G\mu)^{7/2}, \tag{30}$$

or, expressed in terms of the critical temperature T_c ,

$$\frac{T}{T_c} > \lambda^{1/4} \gamma^{3/2} \left(\frac{T}{m_{pl}}\right)^{5/2}. \tag{31}$$

On the other hand, for thermal inflation strings, we obtain

$$\left(\frac{T}{m_{pl}}\right)^2 > \gamma^3 (G\mu)^4, \tag{32}$$

or, after expressing μ in terms of the critical temperature,

$$\frac{T}{T_c} > \gamma^{3/2} \lambda^{-1} \frac{T_c}{m_{pl}}. \tag{33}$$

Comparing these expressions, we see that, for a fixed value of the string tension, cusp annihilation is more important for thermal inflation strings than for Abelian Higgs strings. On the other hand, fixing T_c we see that the importance of cusp annihilation is, maybe surprisingly, less than for Abelian Higgs strings.

Evaluating (31) and (33) at the temperature $T_{eq} \sim 1$ eV of equal matter and radiation (the temperature relevant for cosmological signatures of strings), we see that for Abelian Higgs strings, the cutoff in the loop distribution is determined by cusp annihilation for values $T_c < 10^{10}$ GeV, while for thermal inflation strings, it is for values $T_c < 10^8$ GeV. In particular, for the value $m_0 \sim 10^2\text{--}10^3$ GeV assumed in the original thermal inflation paper [2], we conclude that the cutoff in the loop distribution is given by the cusp annihilation process.

4. Constraints from Cosmological Observations

In this section, we study what constraints on the symmetry breaking scale m_0 of thermal inflation can be derived from cosmological observations. Cosmic strings leave behind interesting signals in many observational windows. In most cases, the effects are gravitational, and hence, the magnitude of the string signal depends on $G\mu$. In terms of $G\mu$, the strength of the signals will, hence, be the same for Abelian Higgs and thermal inflation strings. However, since the relation between T_c and μ is different, the magnitude of the string signals as a function of T_c will change. As the string network consists of both long strings and loops, each will induce specific signatures. Note that in this section, we do not discuss new cosmological signals, but rather the differences in the constraints on the cosmic string parameters between thermal inflation strings and Abelian Higgs strings which these signals imply.

We first turn to signatures of the long string network. For example, long strings lead to line discontinuities in cosmic microwave background (CMB) anisotropy maps [37,38]. This is due to the fact that a long straight string produces a conical deformation of the metric with a deficit angle proportional to $G\mu$ [39]. The magnitude of this signal depends on $G\mu$. The studies of [40,41] show that experiments with the specifications of the South Pole Telescope or the Atacama Cosmology Telescope can constrain the string tension to be

$$G\mu < 10^{-8}. \tag{34}$$

A slightly weaker bound of

$$G\mu < 10^{-7} \tag{35}$$

can be derived from the angular power spectrum of CMB anisotropies [42–44]. The resulting bound on T_c for thermal inflation strings is parametrically stronger than for Abelian Higgs strings, namely

$$\frac{T_c}{m_{pl}} < \lambda^{1/2} 10^{-7}. \tag{36}$$

This bound is obviously satisfied for the value $T_c \sim m_0 = 10^2\text{--}10^3$ GeV assumed in [2].

For Abelian Higgs strings, there is a tighter bound of

$$G\mu < 10^{-10} \quad (37)$$

which comes from the upper bound on the stochastic background of gravitational waves from pulsar timing array measurements [45,46]. This bound depends on having a scaling distribution of loops down to the gravitational radiation cutoff R_g . This bound remains valid for thermal inflation strings since, as the discussion at the end of the previous section showed, cusp annihilation only changes the loop distribution for values of $G\mu$ which are lower than the above bound.

Long strings moving through space produce overdense regions in their wake [47–50]. CMB photons passing through these wakes get absorbed at the 21 cm wavelength. Long cosmic strings hence lead to distinct signals in high redshift 21 cm surveys [51]: wedges of absorption in 21 cm redshift maps which are extended in the angular directions and narrow in redshift direction. The study of [52] shows that the string signal can be detected by surveys such as the MWA telescope down to a value of $G\mu$ comparable to that of (34), and prospects indicate that with better analysis tools, a significant improvement in this bound can be expected.

String wakes also lead to rectangles in the sky with induced CMB polarization (including a B-mode component) [53]. From the analysis of [54], it appears, however, that this signal is harder to extract from observations than the 21 cm signal. At lower redshifts, string wakes also lead to planar overdensities of galaxies. These are, however, disrupted by the gravitational effects of the dominant source of fluctuations [55].

Turning now to signatures of cosmic string loops, the gravitational signals are the same for Abelian Higgs strings and thermal inflation strings given the same value of $G\mu$. String loops seed nonlinear structures by gravitational accretion [56–59]. Given the bounds on $G\mu$ discussed above, strings can only play a subdominant role in explaining the nonlinear structures today. However, since strings form nonlinear seeds immediately after their formation, they will dominate the halo mass function at sufficiently early times [60]. They can provide seeds for intermediate and super-massive black holes at high redshifts [61,62]. It has recently been shown [63] that for superconducting cosmic strings, the “Direct Collapse Black Hole” criteria can be satisfied, and that such loops indeed could explain the origin of the observed high redshift super-massive black holes.

Since thermal inflation strings have a greater width than Abelian Higgs strings for a fixed value of T_c , non-gravitational signals from thermal inflation strings may differ from those of Abelian Higgs strings. Specifically, the flux of cosmic rays [64–67] due to cosmic strings will be larger.

5. Conclusions and Discussion

We have pointed out that thermal inflation models lead to the production of a network of cosmic strings. These thermal inflation strings have different properties compared to strings arising in the Abelian Higgs model. Specifically, for a fixed phase transition temperature, thermal inflation strings have a larger mass per unit length, and hence lead to larger gravitational effects.

For thermal inflation strings, the upper bound on the phase transition temperature from cosmological observations is parametrically more stringent than for Abelian Higgs strings. However, for the value of the symmetry breaking scale suggested in [2], the bounds are satisfied.

Author Contributions: The authors contributed equally to all aspects of the project. All authors have read and agreed to the published version of the manuscript.

Funding: The research at McGill is supported in part by funds from NSERC and from the Canada Research Chair program.

Data Availability Statement: This theoretical study did not generate data.

Acknowledgments: RB wishes to thank the Pauli Center and the Institutes of Theoretical Physics and of Particle- and Astrophysics of the ETH for hospitality.

Conflicts of Interest: The authors declare no conflicts of interest.

Notes

- 1 A real scalar field with a symmetry breaking potential would lead to domain walls, a cosmological disaster [5].
- 2 The new term quadratic in T in the formula for the effective potential is the leading term in the one-loop finite temperature effective potential (see e.g., [7,8] for original discussions). As reviewed in [9], the one-loop finite temperature effective potential determines the dynamics of a Gaussian wavepacket state for ϕ in the presence of a thermal bath.
- 3 Thermal inflation strings were briefly considered in Section 5.2 of [18], with a focus on the dependence of the mass per unit length on the expectation value of the scalar field after symmetry breaking. Our discussion covers many more issues. Cosmic strings in theories with a highly suppressed coefficient of the usual $\lambda\phi^4$ symmetry breaking potential were considered in [19]. While some of the implications for the cosmic strings are similar, the setup is very different. Density fluctuations from thermal inflation strings were discussed e.g., in [20,21]. This is not the topic of the present article.
- 4 The absence of a quartic term in the potential is crucial if we are to generate a hierarchy between T_i and T_c .
- 5 Note that some field theory simulations [25] of the Abelian Higgs model indicate that the energy loss required to maintain the scaling distribution of the long string network proceeds mostly by particle emission rather than by the formation of large loops which then decay by gravitational radiation. We are assuming here that the Nambu–Goto simulations [26–32] are correct. These simulations demonstrate the generation of a scaling distribution of string loops as described here.
- 6 To obtain the first line in (23), note that there is of the order one loop per Hubble volume at the time of formation t_f , i.e., $n(R, t_f) \sim t_f^{-3}$, where $t_f = \alpha^{-1}R$. This number density redshifts such that $n(R, t) = n(R, t_f)(\frac{t_f}{t})^2$, making use of the fact that the volume increases as t^2 in the matter era. The second line is obtained by doing an analogous analysis for loops formed in the radiation period, and taking into account that the physical size of a fixed comoving volume increases as $t^{3/2}$ in the radiation phase.
- 7 See [35] for the correction of an error present in the original work of [34].

References

1. Berera, A. Warm inflation. *Phys. Rev. Lett.* **1995**, *75*, 3218–3221. [[CrossRef](#)] [[PubMed](#)]
2. Lyth, D.H.; Stewart, E.D. Thermal inflation and the moduli problem. *Phys. Rev. D* **1996**, *53*, 1784–1798. [[CrossRef](#)] [[PubMed](#)]
3. Coughlan, G.D.; Fischler, W.; Kolb, E.W.; Raby, S.; Ross, G.G. Cosmological Problems for the Polonyi Potential. *Phys. Lett. B* **1983**, *131*, 59–64. [[CrossRef](#)]
4. Ellis, J.R.; Nanopoulos, D.V.; Quiros, M. On the Axion, Dilaton, Polonyi, Gravitino and Shadow Matter Problems in Supergravity and Superstring Models. *Phys. Lett. B* **1986**, *174*, 176–182. [[CrossRef](#)]
5. Zeldovich, Y.B.; Kobzarev, I.Y.; Okun, L.B. Cosmological Consequences of the Spontaneous Breakdown of Discrete Symmetry. *Zh. Eksp. Teor. Fiz.* **1974**, *67*, 3–11.
6. Banks, T.; Seiberg, N. Symmetries and Strings in Field Theory and Gravity. *Phys. Rev. D* **2011**, *83*, 084019. [[CrossRef](#)]
7. Dolan, L.; Jackiw, R. Symmetry Behavior at Finite Temperature. *Phys. Rev. D* **1974**, *9*, 3320–3341. [[CrossRef](#)]
8. Weinberg, S. Gauge and Global Symmetries at High Temperature. *Phys. Rev. D* **1974**, *9*, 3357–3378. [[CrossRef](#)]
9. Brandenberger, R.H. Quantum Field Theory Methods and Inflationary Universe Models. *Rev. Mod. Phys.* **1985**, *57*, 1. [[CrossRef](#)]
10. Kibble, T.W.B. Phase Transitions In The Early Universe. *Acta Phys. Pol. B* **1982**, *13*, 723.
11. Kibble, T.W.B. Some Implications Of A Cosmological Phase Transition. *Phys. Rept.* **1980**, *67*, 183. [[CrossRef](#)]
12. Vilenkin, A.; Shellard, E.P.S. *Cosmic Strings and Other Topological Defects*; Cambridge University Press: Cambridge, UK, 2000.
13. Hindmarsh, M.B.; Kibble, T.W.B. Cosmic strings. *Rept. Prog. Phys.* **1995**, *58*, 477. [[CrossRef](#)]
14. Brandenberger, R.H. Topological defects and structure formation. *Int. J. Mod. Phys. A* **1994**, *9*, 2117. . [[CrossRef](#)]
15. Durrer, R.; Kunz, M.; Melchiorri, A. Cosmic structure formation with topological defects. *Phys. Rept.* **2002**, *364*, 1. [[CrossRef](#)]
16. Nielsen, H.B.; Olesen, P. Vortex Line Models for Dual Strings. *Nucl. Phys. B* **1973**, *61*, 45–61. [[CrossRef](#)]
17. Brandenberger, R.H. Searching for Cosmic Strings in New Observational Windows. *Nucl. Phys. B Proc. Suppl.* **2014**, *246–247*, 45–57. [[CrossRef](#)]
18. Barreiro, T.; Copeland, E.J.; Lyth, D.H.; Prokopec, T. Some aspects of thermal inflation: The Finite temperature potential and topological defects. *Phys. Rev. D* **1996**, *54*, 1379–1392. [[CrossRef](#)] [[PubMed](#)]
19. Perkins, W.B.; Davis, A.C. Cosmic strings in low mass Higgs cosmology. *Phys. Lett. B* **1998**, *428*, 254–262. [[CrossRef](#)]
20. Bastero-Gil, M.; Gomes, J.M.; Rosa, J.G. Thermal curvature perturbations in thermal inflation. *arXiv* **2023**, arXiv:2301.11666.
21. Kawasaki, M.; Takahashi, T.; Yokoyama, S. Density Fluctuations in Thermal Inflation and Non-Gaussianity. *JCAP* **2009**, *12*, 012. [[CrossRef](#)]
22. Copeland, E.J.; Kibble, T.W.B.; Austin, D. Scaling solutions in cosmic string networks. *Phys. Rev. D* **1992**, *45*, 1000. . [[CrossRef](#)] [[PubMed](#)]
23. Perivolaropoulos, L. COBE versus cosmic strings: An Analytical model. *Phys. Lett. B* **1993**, *298*, 305. [[CrossRef](#)]

24. Austin, D.; Copeland, E.J.; Kibble, T.W.B. Evolution of cosmic string configurations. *Phys. Rev. D* **1993**, *48*, 5594. [[CrossRef](#)]
25. Hindmarsh, M.; Lizarraga, J.; Urrestilla, J.; Daverio, D.; Kunz, M. Scaling from gauge and scalar radiation in Abelian Higgs string networks. *arXiv* **2017**, arXiv:1703.06696.
26. Ringeval, C.; Sakellariadou, M.; Bouchet, F. Cosmological evolution of cosmic string loops. *JCAP* **2007**, *0702*, 023. [[CrossRef](#)]
27. Vanchurin, V.; Olum, K.D.; Vilenkin, A. Scaling of cosmic string loops. *Phys. Rev. D* **2006**, *74*, 063527. [[CrossRef](#)]
28. Lorenz, L.; Ringeval, C.; Sakellariadou, M. Cosmic string loop distribution on all length scales and at any redshift. *JCAP* **2010**, *1010*, 003. [[CrossRef](#)]
29. Blanco-Pillado, J.J.; Olum, K.D.; Shlaer, B. Large parallel cosmic string simulations: New results on loop production. *Phys. Rev. D* **2011**, *83*, 083514. [[CrossRef](#)]
30. Blanco-Pillado, J.J.; Olum, K.D.; Shlaer, B. The number of cosmic string loops. *Phys. Rev. D* **2014**, *89*, 023512. [[CrossRef](#)]
31. Auclair, P.; Ringeval, C.; Sakellariadou, M.; Steer, D. Cosmic string loop production functions. *JCAP* **2019**, *1906*, 015. [[CrossRef](#)]
32. Blanco-Pillado, J.J.; Olum, K.D. Direct determination of cosmic string loop density from simulations. *Phys. Rev. D* **2020**, *101*, 103018. [[CrossRef](#)]
33. Vachaspati, T.; Vilenkin, A. Gravitational Radiation from Cosmic Strings. *Phys. Rev. D* **1985**, *31*, 3052. [[CrossRef](#)]
34. Brandenberger, R.H. On the Decay of Cosmic String Loops. *Nucl. Phys. B* **1987**, *293*, 812. [[CrossRef](#)]
35. Blanco-Pillado, J.J.; Olum, K.D. The Form of cosmic string cusps. *Phys. Rev. D* **1999**, *59*, 063508. [[CrossRef](#)]
36. Kibble, T.W.B.; Turok, N. Selfintersection of Cosmic Strings. *Phys. Lett.* **1982**, *116B*, 141. [[CrossRef](#)]
37. Kaiser, N.; Stebbins, A. Microwave Anisotropy Due To Cosmic Strings. *Nature* **1984**, *310*, 391. [[CrossRef](#)]
38. Moessner, R.; Perivolaropoulos, L.; Brandenberger, R.H. A Cosmic string specific signature on the cosmic microwave background. *Astrophys. J.* **1994**, *425*, 365. [[CrossRef](#)]
39. Vilenkin, A. Gravitational Field of Vacuum Domain Walls and Strings. *Phys. Rev. D* **1981**, *23*, 852–857. [[CrossRef](#)]
40. Hergt, L.; Amara, A.; Brandenberger, R.; Kacprzak, T.; Refregier, A. Searching for Cosmic Strings in CMB Anisotropy Maps using Wavelets and Curvelets. *JCAP* **2017**, *06*, 004. [[CrossRef](#)]
41. McEwen, J.D.; Feeney, S.M.; Peiris, H.V.; Wiaux, Y.; Ringeval, C.; Bouchet, F.R. Wavelet-Bayesian inference of cosmic strings embedded in the cosmic microwave background. *Mon. Not. R. Astron. Soc.* **2017**, *472*, 4081–4098. [[CrossRef](#)]
42. Charnock, T.; Avgoustidis, A.; Copeland, E.J.; Moss, A. CMB constraints on cosmic strings and superstrings. *Phys. Rev. D* **2016**, *93*, 123503. [[CrossRef](#)]
43. Dvorkin, C.; Wyman, M.; Hu, W. Cosmic String constraints from WMAP and the South Pole Telescope. *Phys. Rev. D* **2011**, *84*, 123519. [[CrossRef](#)]
44. Ade, P.A.R. et al. [Planck Collaboration]. Planck 2013 results. XXV. Searches for cosmic strings and other topological defects. *Astron. Astrophys.* **2014**, *571*, A25.
45. Blanco-Pillado, J.J.; Olum, K.D.; Siemens, X. New limits on cosmic strings from gravitational wave observation. *Phys. Lett. B* **2018**, *778*, 392. [[CrossRef](#)]
46. Arzoumanian, Z. et al. [NANOGrav Collaboration]. NANOGrav 11-Year Data Set: Pulsar-Timing Constraints Stoch. Gravitational-Wave Background. *Astrophys. J.* **2018**, *859*, 47. [[CrossRef](#)]
47. Silk, J.; Vilenkin, A. Cosmic Strings And Galaxy Formation. *Phys. Rev. Lett.* **1984**, *53*, 1700. [[CrossRef](#)]
48. Rees, M.J. Baryon concentrations in string wakes at $z \gtrsim 200$: Implications for galaxy formation and large-scale structure. *Mon. Not. R. Astron. Soc.* **1986**, *222*, 27. [[CrossRef](#)]
49. Vachaspati, T. Cosmic Strings and the Large-Scale Structure of the Universe. *Phys. Rev. Lett.* **1986**, *57*, 1655. [[CrossRef](#)] [[PubMed](#)]
50. Stebbins, A.; Veeraraghavan, S.; Brandenberger, R.H.; Silk, J.; Turok, N. Cosmic String Wakes. *Astrophys. J.* **1987**, *322*, 1. [[CrossRef](#)]
51. Brandenberger, R.H.; Danos, R.J.; Hernandez, O.F.; Holder, G.P. The 21 cm Signature of Cosmic String Wakes. *JCAP* **2010**, *1012*, 028. [[CrossRef](#)]
52. Maibach, D.; Brandenberger, R.; Crichton, D.; Refregier, A. Extracting the signal of cosmic string wakes from 21-cm observations. *Phys. Rev. D* **2021**, *104*, 123535. [[CrossRef](#)]
53. Danos, R.J.; Brandenberger, R.H.; Holder, G. A Signature of Cosmic Strings Wakes in the CMB Polarization. *Phys. Rev. D* **2010**, *82*, 023513. [[CrossRef](#)]
54. Blamart, M.; Fronenberg, H.; Brandenberger, R. Signal of cosmic strings in cross-correlation of 21-cm redshift and CMB polarization maps. *JCAP* **2022**, *11*, 012. [[CrossRef](#)]
55. da Cunha, D.C.N.; Harnois-Deraps, J.; Brandenberger, R.; Amara, A.; Refregier, A. Dark Matter Distribution Induced by a Cosmic String Wake in the Nonlinear Regime. *Phys. Rev. D* **2018**, *98*, 083015. [[CrossRef](#)]
56. Vilenkin, A. Cosmological Density Fluctuations Produced by Vacuum Strings. *Phys. Rev. Lett.* **1981**, *46*, 1169; Erratum in *Phys. Rev. Lett.* **1981**, *46*, 1496. [[CrossRef](#)]
57. Turok, N.; Brandenberger, R.H. Cosmic Strings And The Formation Of Galaxies And Clusters Of Galaxies. *Phys. Rev. D* **1986**, *33*, 2175. [[CrossRef](#)] [[PubMed](#)]
58. Sato, H. Galaxy Formation by Cosmic Strings. *Prog. Theor. Phys.* **1986**, *75*, 1342. [[CrossRef](#)]
59. Stebbins, A. Cosmic Strings and Cold Matter. *Astrophys. J. (Lett.)* **1986**, *303*, L21. [[CrossRef](#)]
60. Jiao, H.; Brandenberger, R.; Refregier, A. Early structure formation from cosmic string loops in light of early JWST observations. *Phys. Rev. D* **2023**, *108*, 043510. [[CrossRef](#)]

61. Bramberger, S.F.; Brandenberger, R.H.; Jreidini, P.; Quintin, J. Cosmic String Loops as the Seeds of Super-Massive Black Holes. *JCAP* **2015**, *1506*, 007. [[CrossRef](#)]
62. Brandenberger, R.; Cyr, B.; Jiao, H. Intermediate mass black hole seeds from cosmic string loops. *Phys. Rev. D* **2021**, *104*, 123501. [[CrossRef](#)]
63. Cyr, B.; Jiao, H.; Brandenberger, R. Massive black holes at high redshifts from superconducting cosmic strings. *Mon. Not. R. Astron. Soc.* **2022**, *517*, 2221–2230. [[CrossRef](#)]
64. MacGibbon, J.H.; Brandenberger, R.H. Gamma-ray signatures from ordicosmic strings. *Phys. Rev. D* **1993**, *47*, 2283. [[CrossRef](#)] [[PubMed](#)]
65. MacGibbon, J.H.; Brandenberger, R.H. High-energy neutrino flux from ordinary cosmic strings. *Nucl. Phys. B* **1990**, *331*, 153. [[CrossRef](#)]
66. Hill, C.T.; Schramm, D.N.; Walker, T.P. Ultrahigh-Energy Cosmic Rays from Superconducting Cosmic Strings. *Phys. Rev. D* **1987**, *36*, 1007. [[CrossRef](#)]
67. Wichoski, U.F.; MacGibbon, J.H.; Brandenberger, R.H. High-energy neutrinos, photons and cosmic ray fluxes from VHS cosmic strings. *Phys. Rev. D* **2002**, *65*, 063005. [[CrossRef](#)]

Disclaimer/Publisher’s Note: The statements, opinions and data contained in all publications are solely those of the individual author(s) and contributor(s) and not of MDPI and/or the editor(s). MDPI and/or the editor(s) disclaim responsibility for any injury to people or property resulting from any ideas, methods, instructions or products referred to in the content.